

## Observation of Electromagnetic Shock Waves from Propagating Surface-Dipole Distributions

Ch. Fattinger and D. Grischkowsky

IBM Watson Research Center, P.O. Box 218, Yorktown Heights, New York 10598

(Received 27 January 1989)

We have directly measured the time-dependent electromagnetic shock wave generated by an electric surface-dipole distribution propagating faster than the phase velocity in the underlying dielectric substrate. The results are in good agreement with a theory describing the moving volume-dipole distribution with the inclusion of an equal strength surface reflection.

PACS numbers: 41.10.-j, 03.50.-z, 84.40.-x

In a recent experiment,<sup>1</sup> evidence was presented which indicated that an electromagnetic shock wave is produced when an ultrashort electric pulse propagates on a coplanar transmission line at speeds faster than the phase velocity in the underlying dielectric substrate. Because these electrical pulses propagate as the differential (TEM) mode of the two-line coplanar transmission line, there is a positive pulse on one line and a negative pulse of identical shape on the other. Therefore, the total electric field of the pulse is described by a propagating electrical dipole distribution. Consequently, as seen from the underlying dielectric, the situation is that of an electric dipole distribution propagating on the surface faster than the phase velocity in the dielectric. This situation produces an electromagnetic shock wave in a manner similar to Cherenkov radiation<sup>2</sup> and electro-optic Cherenkov radiation.<sup>3-5</sup> The initial indirect observation<sup>1</sup> was the measurement of the frequency-dependent loss from the propagating electric pulse due to the Cherenkov radiation. In this Letter we present the first direct observation of the shock wave and a measurement of its time dependence. In addition, we obtain good agreement between our experiment and a new theoretical result.

Because our physical situation is related to electro-optic Cherenkov radiation, we briefly review this earlier work. Auston created a moving volume electric dipole distribution by driving the optical rectification effect in a nonlinear dielectric material with an ultrashort laser pulse.<sup>3,4</sup> Because the speed in the dielectric for both the visible light pulse and the volume dipole was much faster than the phase velocity for the THz frequencies describing the electric field of the volume-dipole distribution, an electromagnetic shock wave was produced. For a laser pulse focused to transverse dimensions smaller than the spatial pulse length, Kleinman and Auston (KA) have calculated the time-dependent electric field of the shock wave.<sup>5</sup>

In the limit as a time-dependent dipole inside a dielectric approaches the dielectric surface to arbitrarily small distances, the emitted radiation remains the vector sum of the field radiated into the dielectric and the field reflected from the surface.<sup>6,7</sup> For a time-dependent di-

pole oriented parallel to the surface, both the total radiated power and the angular distribution of radiation are continuous as the dipole is moved across the surface; the solution of the electromagnetic boundary-value problem is the same for the dipole located either in the proximity of the surface or on the surface.<sup>7</sup> When the dipole is some distance away from the surface, the resulting so-called "wide-angle interference" depends on the magnitude and the relative phase of the reflected radiation and on the optical path difference between the interfering waves. As the distance between the dipole and the surface approaches zero, the phase difference between the two waves is due only to the reflection. Using this theoretical approach, we obtain the time dependence and the spatial distribution of the electromagnetic field generated by the propagating surface-dipole distribution.

These results will now be applied to the situation illustrated in Fig. 1, after a brief description of the experimental parameters. The index of refraction  $n_0$  for the ordinary ray in the sapphire substrate is approximately constant at 3.07 from low frequencies up to more than 1 THz.<sup>8</sup> The corresponding group velocity of the electrical pulse and the associated surface-dipole distribution on the transmission line is  $v_g = c/2.28$ .<sup>9</sup> Given  $n_0$  and  $v_g$ , we calculate the angle  $\theta_0$  of the (ordinary) shock wave to be  $42^\circ$ .<sup>5</sup> Therefore, the shock wave hits the sapphire/air interface at an angle of incidence well above the critical angle  $\alpha_c = 19^\circ$  for total internal reflection. This complete reflection at the interface changes the shock wave due to the accompanying phase shift  $\Phi$ .<sup>10</sup> The reflected and directly emitted shock waves (Cherenkov cones) spatially coincide. Therefore, our predicted shock wave is the sum of two equal-strength time-dependent terms, the directly radiated electric field  $E_D$  with the KA time dependence<sup>5</sup> shown in Fig. 2(a), and the reflected field  $E_R$  with a different time dependence due to its total reflection. Before reflection, the  $E_R$  term also had the KA time dependence. Because the radiation emitted from the surface-dipole distribution is highly directional,<sup>6</sup> only those conical rays emitted in directions close to the two rays shown in Fig. 1(b) have significant amplitudes. For the ordinary ray propagating in the  $x$ - $z$  plane

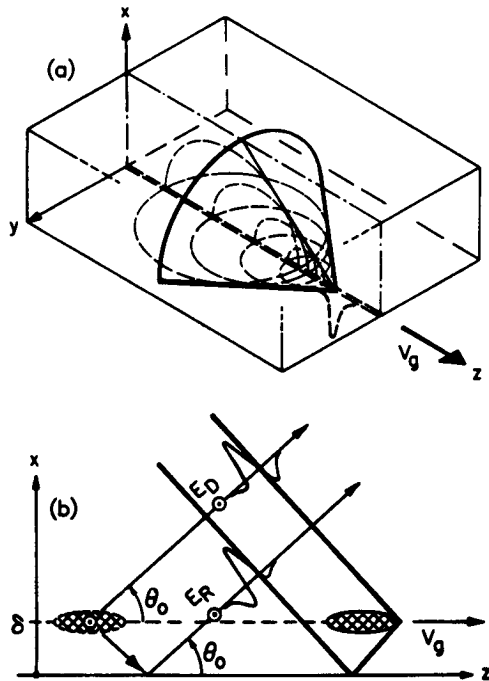


FIG. 1. (a) Cherenkov cone (shock wave) in the dielectric half-space for the propagating surface-dipole distribution. (b) Cross-sectional view of the directly radiated and reflected Cherenkov cones from a moving volume-dipole distribution near the surface of a dielectric.

as shown in Fig. 1(b), the phase shift upon reflection is  $\Phi_0 = -89.8^\circ$  for all the frequency components of the pulse.<sup>11</sup> This phase shift changes the shock wave of Fig. 2(a) to that of Fig. 2(b). The predicted freely propagating shock wave shown in Fig. 2(c) is the sum of Figs. 2(a) and 2(b). This situation is depicted in Fig. 1(b) as the sum of  $E_D$  and  $E_R$  in the limit as  $\delta$  approaches zero. The sum is equivalent to a phase shift of the KA solution by  $\Phi_0/2$ , together with an amplitude change of  $2\cos(\Phi_0/2)$ .

The observation of the shock wave was made possible by the focusing geometry illustrated in Fig. 3(a). A section of a crystalline sapphire cylinder is contacted to the backside (sapphire side) of the silicon-on-sapphire (SOS) wafer used to generate the shock wave. Because sapphire is strongly birefringent at THz frequencies with refractive indices of  $n_o = 3.07$  for the ordinary ray and  $n_e = 3.41$  for the extraordinary ray, two shock waves with orthogonal polarization and propagating with different speeds are emitted into the sapphire.<sup>12</sup> The cylindrical symmetry of the experimental configuration preserves, during reflection from the cylindrical mirror, the orthogonal polarization of the ordinary and extraordinary shock waves, which are polarized perpendicular and parallel to the plane of incidence, respectively. As indicated in Fig. 3, the cylindrical mirror focuses shock-wave radiation on the detection gap from only one point on the line, the emission point. The excitation site was 7.1 mm

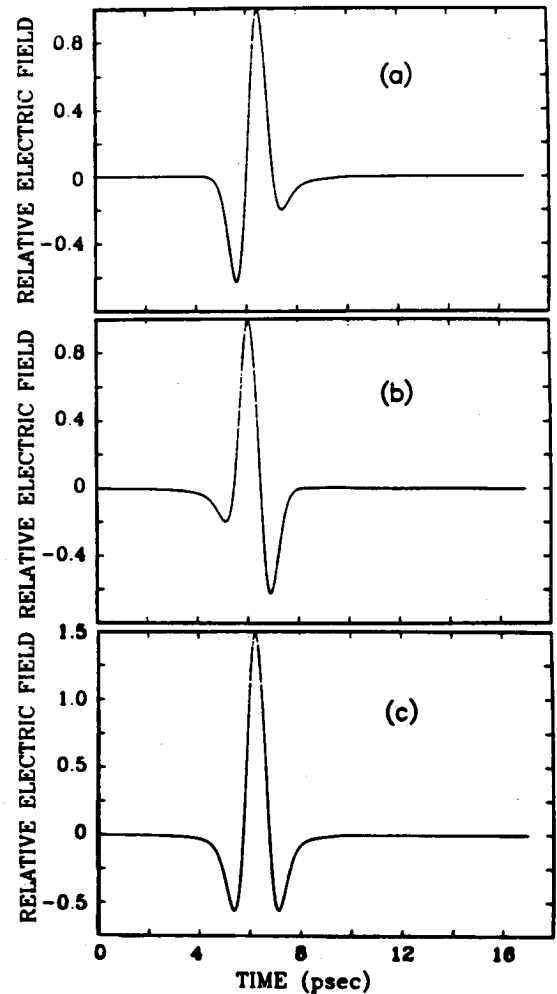


FIG. 2. (a) The Kleinman-Auston (KA) solution for the volume-dipole distribution shock wave. (b) The KA solution after a phase shift of  $\Phi_0 = -89.8^\circ$  for all frequencies. (c) The surface-dipole distribution shock wave, the sum of (a) and (b).

from the gap and was located outside of the sapphire cylinder in order to prevent the cylinder from collecting the burst of radiation accompanying the creation of the electrical pulse on the transmission line.<sup>13</sup> Knowing  $\Theta_0$  and the 5.1-mm diam of the cylinder, we obtain 5.6 mm for the separation between the emission point and the detection gap, and 7.4 mm for the total free-flight distance of the focused ordinary shock wave.

The coplanar transmission-line structure<sup>1,9</sup> used to generate the ultrashort electrical pulses is designated as the generation line in Fig. 3(c). By photoconductively shorting the charged line at the excitation site with the excitation beam of 70-fsec pulses from a colliding pulse mode-locked dye laser, subpicosecond electrical pulses are produced. This method of pulse generation ensures a pure dipolar pulse<sup>9</sup> with a field distribution which matches the differential (TEM) mode of the coplanar line. The resulting electrical pulses propagating on the generation line are measured by a fast photoconductive switch, driven by the time-delayed monitor beam of the

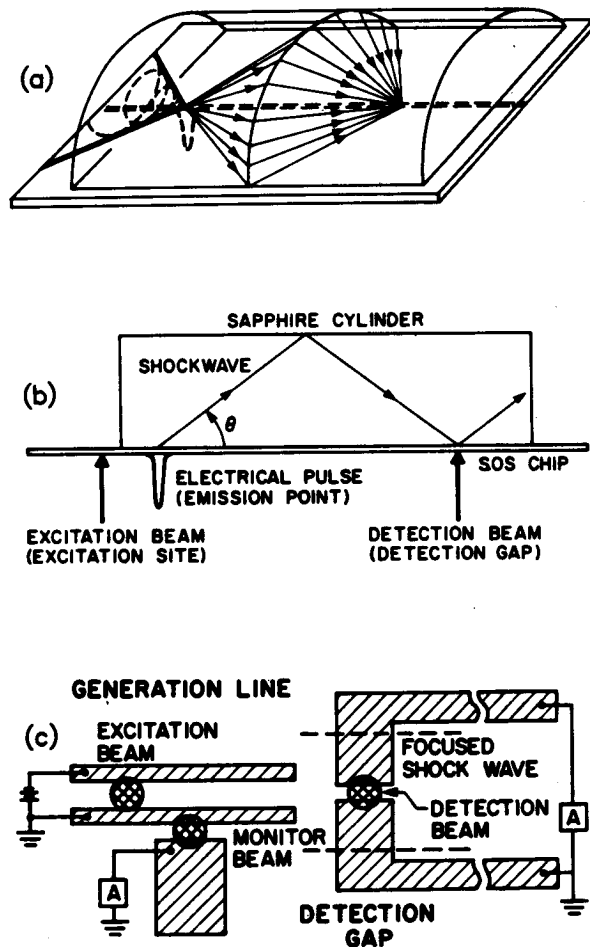


FIG. 3. (a) Focusing optics for the shock wave. (b) Cross-sectional view of the focusing optics. (c) Schematic diagram of the charged coplanar transmission line and the detection gap.

same 70-fsec laser pulses. The generation line consisted of two parallel 5- $\mu\text{m}$ -wide, 1- $\mu\text{m}$ -thick, aluminum lines separated from each other by 10  $\mu\text{m}$ . Typically, the bias voltage was 10 V. The shock wave is measured with the detection gap, separated by 1 mm from the generation line. The shock wave electrically biases the gap, which is driven by the detection beam. The detection-gap spacing was 5  $\mu\text{m}$  with a width of 20  $\mu\text{m}$ . The gap itself was at the end of a second transmission line consisting of two parallel 10- $\mu\text{m}$ -wide, 1- $\mu\text{m}$ -thick aluminum lines separated from each other by 30  $\mu\text{m}$ . Both transmission lines were fabricated on an undoped-SOS wafer, heavily implanted with  $\text{O}^+$  ions.

Figure 4(a) displays the measured 1.2-psec (FWHM) electrical pulse on the generation line. Considering the relatively slow 0.7-psec response time of the monitor side gap, we estimate that the actual (FWHM) pulse width was approximately 1.0 psec. For this result the spatial separation between the exciting and sampling beams was 1.5 mm, equal to the separation between the excitation site and the emission point.

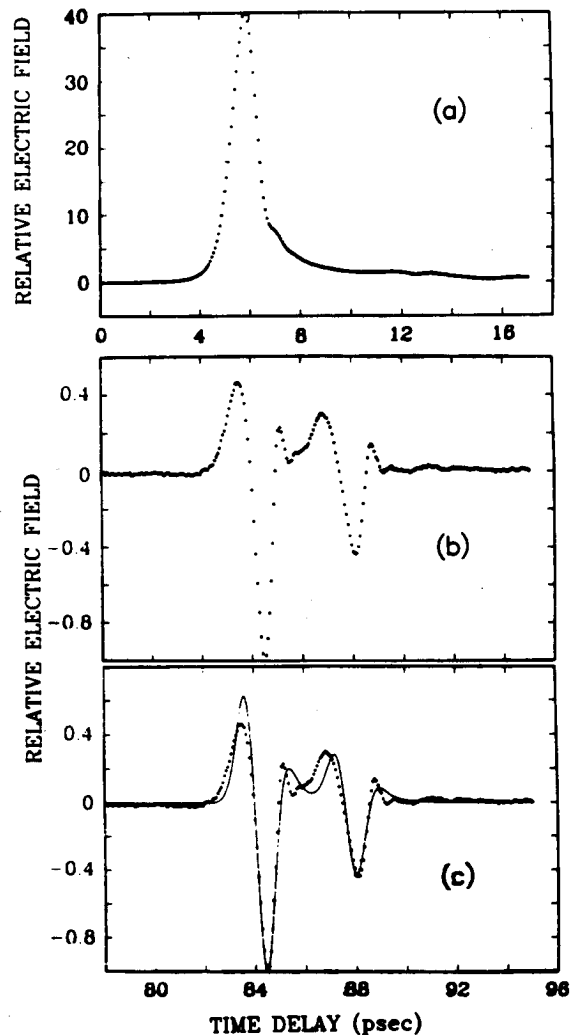


FIG. 4. (a) Measured electrical pulse on the transmission line. (b) Measured focused electromagnetic shock waves. (c) Measured shock waves compared with theory.

The measured electric field of the focused shock wave is shown in Fig. 4(b), where the 78-psec delay indicates the propagation time from the emission point to the detection gap. The amplitude is normalized relative to the 40 $\times$  larger pulse on the line [Fig. 4(a)]. The observed time dependence is exceptionally fast with well resolved features down to the 0.5-psec response time of the detection gap. This measurement is the sum of four 2-min scans of the relative time delay of the detection beam; the resulting signal-to-noise ratio is better than 100:1. The appearance of two similar shock waves is due to the birefringence of sapphire. The first is the ordinary shock wave while the second, arriving 3.6-psec later, is the extraordinary shock wave.<sup>12</sup>

In order to compare experiment and theory, we now explain how our predicted shock wave is changed to the inverted KA solution by the two total internal reflections shown in Fig. 3(b). When the emergent (ordinary)

shock wave hits the cylindrical mirror, it is totally reflected; all its spectral components are phase shifted by  $\Phi_0$ , and the time dependence is changed. This reflection focuses the wave on the detector where another total reflection occurs. The detector measures the total field, the sum of the incident and equal strength reflected wave (phase shifted by  $\Phi_0$ ), with the net phase shift of  $\Phi_0/2$ . In summary, the initial shock wave of Fig. 2(c) is equivalent to the KA solution with a  $\Phi_0/2$  phase shift. This wave is then phase shifted  $\Phi_0$  by the mirror and  $\Phi_0/2$  at the detector. Consequently, the total phase shift is  $2\Phi_0$  which is approximately equal to  $-\pi$ . Thus, the observed shock wave should be the inverted KA solution. For the extraordinary shock wave three different planes of incidence must be considered. The phase shifts of approximately  $-180^\circ$  for the emission point and detection gap have almost no effect on the time dependence due to the relative polarization of the directly emitted and reflected components. Thus, the emergent extraordinary shock wave has the original KA time dependence. The total reflection at the cylindrical mirror shifts the phase by  $-170^\circ$ , which remains as the net phase shift at the detection gap. Therefore, the inverted KA dependence is also predicted for the measured extraordinary shock wave.

In Fig. 4(c), the measurements are compared with the inverted KA result for two overlapping shock waves separated by 3.6 psec.<sup>12</sup> The relative strengths of these waves have been adjusted for the best fit to be 1:0.4, indicating the different radiation and detection efficiencies for the ordinary and extraordinary shock waves, respectively. They both correspond to the radiation from 0.65-psec  $1/e$  half-width, or equivalently 1.1-psec FWHM, Gaussian dipolar electrical pulses moving on the transmission line with  $v_g = c/2.28$ . The 1.1-psec pulse width is only slightly longer than our measured value of 1.0 psec for the electrical pulse propagating on the transmission line. Even though the above analysis neglects several minor complicating effects,<sup>14</sup> the agreement between theory and experiment is quite good. In summary, the measurements have verified the existence of the shock wave produced by the propagating surface-dipole distribution, and the agreement between theory and experiment for the time dependence has confirmed the importance of the surface reflection. In addition, this

shock-wave radiation is a fundamental limitation for the propagation of ultrafast signals as surface waves.

We acknowledge Martin van Exter and Joshua E. Rothenberg for stimulating and clarifying discussions. This research was partially supported by the U. S. Office of Naval Research.

<sup>1</sup>D. Grischkowsky, I. N. Duling, III, J. C. Chen, and C.-C. Chi, *Phys. Rev. Lett.* **59**, 1663 (1987).

<sup>2</sup>J. V. Jelley, *Cherenkov Radiation and Its Applications* (Pergamon, New York, 1958).

<sup>3</sup>D. H. Auston, *Appl. Phys. Lett.* **43**, 713 (1983).

<sup>4</sup>D. H. Auston, K. P. Cheung, J. A. Valdmanis, and D. A. Kleinman, *Phys. Rev. Lett.* **53**, 1555 (1984).

<sup>5</sup>D. A. Kleinman and D. H. Auston, *IEEE J. Quantum Electron.* **20**, 964 (1984).

<sup>6</sup>W. Lukosz, *J. Opt. Soc. Am.* **69**, 1495 (1979).

<sup>7</sup>W. Lukosz, *Phys. Rev. B* **22**, 3030 (1980).

<sup>8</sup>E. E. Russell and E. E. Bell, *J. Opt. Soc. Am.* **57**, 543 (1967).

<sup>9</sup>D. Grischkowsky, M. B. Ketchen, C.-C. Chi, I. N. Duling, III, N. J. Halas, J.-M. Halbout, and P. G. May, *IEEE J. Quantum Electron.* **24**, 221 (1988).

<sup>10</sup>K. P. Cheung and D. H. Auston, *Opt. Lett.* **10**, 218 (1985).

<sup>11</sup>M. Born and E. Wolf, *Principles of Optics* (Pergamon, Oxford, 1980), 6th ed.; see Chap. 1.5.4, p. 49, Eqs. (59) and (60). Birefringent media are treated in the original work of F. Pockels, *Lehrbuch der Kristallographie* (Teubner, Berlin, 1906).

<sup>12</sup>With the  $c$  axis of both the cylinder and the wafer parallel to the transmission line, the extraordinary shock wave has a cylindrical shape and the Cherenkov angle  $\theta_c$  is given by  $\tan\theta_c = (n_0/n_e)\tan\theta_0$ . For the extraordinary shock wave the conical rays are no longer perpendicular to the wave surface and have the phase velocity

$$v_c = (c/n_e)[\sin^2\theta_c + (n_0/n_e)^2\cos^2\theta_c]^{-1/2}.$$

This yields a 3.8-psec delay (in agreement with experiment) of the extraordinary shock wave relative to the ordinary wave at the detection gap.

<sup>13</sup>Ch. Fattinger and D. Grischkowsky, *Appl. Phys. Lett.* **53**, 1480 (1988).

<sup>14</sup>These effects are (1) a weak frequency dependence of  $n_0$  and  $n_e$ , (2) a slight reshaping of the pulse as it approaches the focal line of the cylindrical mirror (Guoy effect for cylindrical focusing), and (3) the higher frequencies are focused more tightly as  $\omega^{1/2}$ .